

Cell wall ester modifications and volatile emission signatures of plant response to abiotic stress

Kolby J. Jardine¹  | Rebecca A. Dewhirst¹ | Suman Som¹ | Joseph Lei¹ | Eliana Tucker¹ | Robert P. Young²  | Miguel Portillo-Estrada³  | Yu Gao⁴ | Luping Su⁵ | Silvano Fares^{6,7} | Cristina Castanha¹ | Henrik V. Scheller^{4,8} | Jenny C. Mortimer^{4,9}

¹Lawrence Berkeley National Lab, Climate and Ecosystem Science Division, Berkeley, California, USA

²Environmental Molecular Sciences Laboratory, Pacific Northwest National Lab, Richland, Washington, USA

³Department of Biology, Research group PLECO (Plants and Ecosystems), University of Antwerp, Wilrijk, Belgium

⁴Lawrence Berkeley National Lab, Joint BioEnergy Institute, Emeryville, California, USA

⁵Tofwerk USA, Boulder, Colorado, USA

⁶Institute of BioEconomy, National Research Council, Rome, Italy

⁷Department of Environmental Science, Policy, and Management, University of California, Berkeley, California, USA

⁸Department of Plant and Microbial Biology, University of California, Berkeley, California, USA

⁹School of Agriculture, Food, and Wine, University of Adelaide, Glen Osmond, South Australia, Australia

Correspondence

Kolby J. Jardine, Lawrence Berkeley National Lab, Climate and Ecosystem Science Division, Berkeley, CA 94720, USA.
Email: kjjardine@lbl.gov

Funding information

US Department of Energy

Abstract

Growth suppression and defence signalling are simultaneous strategies that plants invoke to respond to abiotic stress. Here, we show that the drought stress response of poplar trees (*Populus trichocarpa*) is initiated by a suppression in cell wall derived methanol (MeOH) emissions and activation of acetic acid (AA) fermentation defences. Temperature sensitive emissions dominated by MeOH (AA/MeOH <30%) were observed from physiologically active leaves, branches, detached stems, leaf cell wall isolations and whole ecosystems. In contrast, drought treatment resulted in a suppression of MeOH emissions and strong enhancement in AA emissions together with volatiles acetaldehyde, ethanol, and acetone. These drought-induced changes coincided with a reduction in stomatal conductance, photosynthesis, transpiration, and leaf water potential. The strong enhancement in AA/MeOH emission ratios during drought (400%–3500%) was associated with an increase in acetate content of whole leaf cell walls, which became significantly ¹³C₂-labelled following the delivery of ¹³C₂-acetate via the transpiration stream. The results are consistent with both enzymatic and nonenzymatic MeOH and AA production at high temperature in hydrated tissues associated with accelerated primary cell wall growth processes, which are downregulated during drought. While the metabolic source(s) require further investigation, the observations are consistent with drought-induced activation of aerobic fermentation driving high rates of foliar AA emissions and enhancements in leaf cell wall O-acetylation. We suggest that atmospheric AA/MeOH emission ratios could be useful as a highly sensitive signal in studies investigating environmental and biological factors influencing growth-defence trade-offs in plants and ecosystems.

Abbreviations: AA, acetic acid; MeOH, methanol; VOCs, volatile organic compounds.

This is an open access article under the terms of the Creative Commons Attribution-NonCommercial-NoDerivs License, which permits use and distribution in any medium, provided the original work is properly cited, the use is non-commercial and no modifications or adaptations are made.

© 2022 The Authors. *Plant, Cell & Environment* published by John Wiley & Sons Ltd.

KEYWORDS

AA/MeOH ratio, aerobic fermentation, cell wall esters, growth suppression, pectin, plant drought stress, xylan

1 | INTRODUCTION

Fast growing trees are increasingly utilized as a sustainable source of bioproducts and biofuels as well as carbon farming, urban greening, hillslope stabilisation and marginal land restoration and re-forestation (Furtado et al., 2014; Ragauskas et al., 2006). Field observations have consistently shown that nonwater limited poplar plantations have high growth and productivity rates, but are highly sensitive to drought (Ji et al., 2020; Zhou et al., 2013). For example, poplar trees in northern China have experienced large-scale dieback and mortality in recent years (Ji et al., 2020). An estimated 79.5% of the area of the poplar forests have experienced severe degradation with an observed trend of narrower tree-ring widths of intact trees together with reduced soil moisture. These observations highlight the need to understand the mechanisms of poplar forest growth suppression and die-back in response to drought stress (Ji et al., 2020). Prolonged excessive water loss via transpiration not replaced by water uptake from the soil can result in drought-induced tissue senescence and mortality, thereby converting individual plants and ecosystems from net sinks of CO₂ to net sources (Jardine et al., 2015; Liu et al., 2021; McDowell et al., 2008). Understanding the biological mechanisms and environmental thresholds that determine plant responses to drought stress is critical for predicting how the structure and function of managed ecosystems will respond to environmental change (Dewhurst et al., 2021; McDowell et al., 2008).

Previous studies have characterized the sequence of plant hydraulic, physiological, biochemical, and structural changes associated with reversible and irreversible responses to drought stress. For example, leaf dehydration responses of ten angiosperm species showed stomatal closure and a decrease in xylem conductance occurring first as a reversible response (Trueba et al., 2019). This was followed by reaching the turgor loss point, xylem embolism, and the cessation of transpiration as a critical irreversible threshold following which further irreversible damage occurred including to the membranes, pigments, and other components of the photochemical system in the chloroplast (Trueba et al., 2019). While ecosystem response to water deficit can be detected by current remote sensing methods such as solar induced fluorescence (SIF) (Sun et al., 2015), and various normalized vegetation indices such as the Normalized Difference Vegetation Index (NDVI) (Peters et al., 2002) and Enhanced Vegetation Index (EVI) (Aulia et al., 2016), these generally only identify extreme drought and the associated irreversible loss of major leaf function such as transpiration and net carbon assimilation. For example, in 2 year old *Populus deltoides* individuals, while strong responses of net photosynthesis and stomatal conductance to initial water stress were observed at the leaf level, SIF showed relatively minimal changes (Helm et al., 2020). It was concluded that the value of SIF as an accurate estimator of net photosynthesis may decrease during

mild stress events of short duration, especially when the response is primarily stomatal and not fully coupled with the degradation of photosynthetic capacity. This highlights the need for new methods to better understand the biochemical, physiological, and ecological mechanisms in situ associated with the onset of drought stress including processes that alter plant growth and defence balances and their associated changes in leaf CO₂ and H₂O gas exchange fluxes.

A common thread among many of the biochemical and physiological processes that determine ecosystem dynamic responses to climate change variables are alterations in plant cell wall chemical composition, structure, and function (Dewhurst, Afseth, et al., 2020; Dewhurst, Mortimer, et al., 2020). A large proportion of the plant cell wall polymers can be heavily modified with methyl and O-acetyl ester groups which may play important roles in cell growth and tissue development (Peaucelle et al., 2012), proper xylem (Yuan et al., 2016) and stomatal functioning (Amsbury et al., 2016), central carbon and energy metabolism (Jardine et al., 2017), and stress communication and signalling (Novaković et al., 2018). For example, wood of hybrid poplar trees, one of the fastest growing temperate trees in the world, is composed of lignin (22%), cellulose (40%), hemicellulose (20%) dominated by the O-acetylated polysaccharide glucuronoxylan, and other polysaccharides such as pectins (18%), which can be both heavily O-acetylated and methyl-esterified (Sannigrahi et al., 2010). The two main components of the plant primary cell wall, the pectin matrix and the cellulose/xyloglucan network, are constantly remodelled to support dynamic morphological and physiological processes from daily growth and stress response patterns, to developmental changes over longer time scales (Chebli & Geitmann, 2017). This remodelling is regulated, in part, by a number of loosening and stiffening agents including pectin and xylan methyl and acetyl esterases which catalyse the hydrolysis of cell wall esters on the wall. The hydrolysis of methyl and O-acetyl esters leads to rapid physicochemical changes in the cell wall and the release of methanol (MeOH) (Fall, 2003) and acetic acid (Scheller, 2017). Given that cell wall methyl and O-acetyl esters are known to modify cell wall elasticity/rigidity (Peaucelle et al., 2011), and previous observations have shown links between bulk cell wall elasticity and water relations (Roig-Oliver et al., 2020), they may play important roles in the response to drought (Ganie & Ahammed, 2021). However, how the degree of cell wall esterification varies with abiotic stress is largely unknown (Gille & Pauly, 2012; Pauly & Keegstra, 2010).

The source of cell wall O-acetyl esters is thought to be primarily acetyl-CoA. Acetyl-CoA is a central component of plant carbon and energy metabolism, generated independently in many organelles such as through the reaction catalysed by pyruvate dehydrogenase (PDH) during aerobic respiration (mitochondria) and fatty acid biosynthesis (chloroplasts). First described as the 'PDH bypass pathway' in yeast, acetyl-CoA

production in plants under aerobic conditions has also been linked to enzymes involved in fermentation like pyruvate decarboxylase and acetaldehyde dehydrogenase (Wei et al., 2009). Recently, acetate accumulation produced by aerobic fermentation during drought stress was shown to coordinate plant response to drought stress through a global reprogramming of transcription, cellular metabolism, hormone defence signalling, and chromatin modification mediated by protein acetylation (Kim et al., 2017).

In this study, we first hypothesize that during rapid growth under well-watered conditions, MeOH and acetic acid (AA) from leaf cell wall ester hydrolysis is the main source of foliar MeOH and AA emission to the atmosphere during well-watered conditions. Moreover, ester hydrolysis reactions increase as a function of temperature through both enzymatic and nonenzymatic ester hydrolysis reactions. Second, we hypothesize that due to hydraulic limitations to growth during drought stress, cell wall-derived MeOH production is inhibited. Together with reductions in stomatal conductance, we predict that drought-induced suppression of growth rates will also suppress leaf MeOH emissions. In contrast to well-watered conditions where cell wall esters are the dominant source of MeOH and AA emissions, we hypothesize that aerobic fermentation becomes the dominant source of leaf AA emissions during drought stress. Finally, in addition to acetate-mediated signalling mechanisms associated with protein acetylation (Kim et al., 2017), we hypothesize that additional biopolymers such as cell wall polysaccharides, may also respond with increased acetylation during drought responses.

We aimed to test these hypotheses by quantifying drought induced changes in bulk leaf cell wall composition as well as *O*-acetylation content in 2-year old potted California poplar (*Populus trichocarpa*) trees. Delivery of 10 mM $^{13}\text{C}_2$ -acetate solutions to canopy leaves via the transpiration stream were used to evaluate the metabolic connection between leaf free acetate and *O*-acetylation of bulk leaf cell wall polysaccharides. During experimental drought stress, we collected real-time patterns in MeOH and AA emissions together with the fermentation volatiles acetaldehyde, ethanol and acetone in parallel with leaf gas exchange (net photosynthesis, transpiration, stomatal conductance) and leaf water potential measurements. Complementary environmental sensitivities of MeOH and AA gas exchange studies are presented on hydrated leaf bulk cell wall preparations and physiologically active leaves, branches and whole ecosystems. We define the AA/MeOH emission ratio as a potentially sensitive atmospheric indicator of environmental and biological conditions that favour rapid plant growth versus suppressed growth and defence activation.

2 | MATERIALS AND METHODS

2.1 | Leaf physiological impacts during an experimental drought

Thirty California poplar (*Populus trichocarpa*) saplings were obtained from a commercial supplier (Plants of the Wild). The trees were

transferred into #2 pots (6.59 L) with Supersoil planting media (Scotts Co) and maintained for 2 years in the UC Berkeley Oxford Tract greenhouse under natural lighting supplemented with LED lighting (6:00–20:00 light period; Lumigrow 325 Pro). The 30 potted trees reached a stem diameter (5 cm) and height (1.5 m) just before the commencement of experimental measurements. A subsection (15 individuals) of the 2-year old trees had water withheld for 1 week (drought plants), while a control group (15 individuals) continued to receive morning, afternoon and night water supply. For each individual throughout the controlled drought experiment, one mature leaf was selected for leaf gas exchange measurements in the greenhouse using a portable Li6800 photosynthesis system including stomatal conductance (g_s , $\text{mol m}^{-2} \text{s}^{-1}$), net photosynthesis (A , $\mu\text{mol m}^{-2} \text{s}^{-1}$), and transpiration (E , $\text{mmol m}^{-2} \text{s}^{-1}$) under standard environmental conditions (400 ppm reference CO_2 , 25 mmol mol^{-1} reference absolute humidity, 1000 $\mu\text{mol m}^{-2} \text{s}^{-1}$ photosynthetically active radiation, 600 $\mu\text{mol s}^{-1}$ leaf chamber air flow rate, 31°C heat exchange block). Immediately following leaf gas exchange measurements in the morning, leaf water potential was determined using a nitrogen pressure chamber instrument (Model 600; PMS Inst). The leaf was detached from the tree using a razor blade, and the petiole sealed in the leaf pressure chamber where nitrogen pressure slowly increased until liquid water was visible from the petiole. Following the gas exchange and leaf water potential measurements, a second mature leaf was taken from each of the 30 trees and frozen on dry ice and stored at -80°C before cell wall analysis. Leaf gas exchange and water potential measurements and frozen leaf samples were collected from one mature leaf for each of the 15 control and 15 drought-treated individuals at time = 0, 1, 4 and 7 days.

2.2 | Leaf alcohol insoluble residue (AIR) preparations

Cell wall preparations (AIR), were extracted from poplar leaf samples collected during the drought and $^{13}\text{C}_2$ -acetate labelling experiments. Leaves were flash frozen in liquid nitrogen and then ground to a powder with a pestle and mortar on dry ice. The ground samples were incubated in 96% (v/v) ethanol at 70°C for 30 min. The supernatant was discarded and the samples washed successively in 100% ethanol, 2:3 chloroform: methanol (twice, with shaking for at least 1 h), 60%, 80% and 100% ethanol. Samples were centrifuged and the supernatant discarded between each washing step. The resulting AIR was dried in a speedvac and destarched for the monosaccharide analyses using amylase, amyloglucosidase and pullulanase (Megazyme Ltd) as previously described (Sechet et al., 2018).

Bulk *O*-acetyl ester content of AIR samples was carried out using a commercial kit (Acetate Assay Kit; BioVision). AIR samples (2.5 mg) were saponified with NaOH (1 M, 125 μl) for 16 h then neutralized with 1 M HCl. The samples were centrifuged (10 min at 15 000 rpm) and 5 μl of the supernatant was transferred to a 96-well plate. The samples were treated with the assay kit enzymes and plates incubated at room temperature for 40 min. Absorbances were

measured at 450 nm on a 96-well plate reader (SpectraMax M2; Molecular Devices). Total O-acetyl content of the AIR samples ($\mu\text{g}/\text{mg}$ AIR) were determined by including a six-point calibration on each plate using the included standard.

To determine bulk leaf cell wall monosaccharide composition, destarched AIR (200 μg) was incubated in 2 M trifluoroacetic acid (400 μl) at 120°C for 3 h. The supernatant was collected after centrifugation. The pellet was washed with 200 μl milliQ water, centrifuged and the supernatant collected. The combined supernatants from each sample were dried in a speedvac. The sample was resuspended in 200 μl milliQ water, filtered on a 0.22 μm centrifuge filtration plate then analysed for monosaccharide composition using high-pressure anion-exchange chromatography (Dionex-ICS 5000; Thermo Fisher Scientific).

2.3 | Real-time AA and MeOH emission measurements

Experimental details of the leaf, branch, and ecosystem gas exchange methods to determine AA and MeOH emissions, as well as the detached stem, detached leaf and hydrated AIR temperature response curves can be found in the supplementary methods. Briefly, emission rates of MeOH and AA were quantified in real-time (roughly 2.5 measurements per minute) using a high sensitivity quadrupole proton transfer reaction mass spectrometer (PTR-MS, Ionicon with a QMZ 422 quadrupole). The PTR-MS was regularly calibrated to a primary standard by dynamic dilution (Supporting Information: Figure S1). AA and MeOH emissions were determined using PTR-MS at the leaf level using an environmentally controlled leaf photosynthesis system (Model 6800; Licor Biosciences), branch level using a custom 5.0 L transparent Tedlar gas exchange enclosure with artificial lighting, and from a temperature-controlled chamber used for detached leaf, stem, and hydrated AIR samples (Model 150 Dynacalibrator, ± 0.01 C temperature accuracy; Vici Metronics). Together with air temperature, continuous above canopy ambient AA and MeOH concentrations during the growing season were made at a poplar plantation in Belgium (Portillo-Estrada et al., 2018), a mixed hardwood forest in Alabama (Su et al., 2016), and above a citrus grove in California (Park et al., 2013). Vertical ecosystem fluxes of MeOH and AA were estimated at the Belgium field site using the technique of eddy covariance employing high frequency vertical wind and MeOH and AA concentration measurements (Portillo-Estrada et al., 2018). While ecosystem concentration and flux measurements MeOH were collected at all three sites using eddy covariance with PTR-TOF-MS, only the Belgium poplar plantation reported ecosystem scale AA flux data. At the Alabama mixed forest site, AA fluxes were not reported (Su et al., 2016) and at the citrus grove in California, AA fluxes were reported to suffer from gaseous AA surface interactions within tubing (Park et al., 2013). Therefore, at the Alabama and California sites, diurnal ambient concentrations of MeOH and AA were analysed instead of fluxes as a function of air temperature.

2.4 | Long-distance $^{13}\text{C}_2$ -acetate transport in the transpiration stream and leaf cell wall O-acetylation interactions

In order to evaluate the possibility of long-distance metabolic interactions between plant tissues mediated by acetate in the transpiration stream, including influencing O-acetylation dynamics of cell walls, $^{13}\text{C}_2$ -acetate labelling studies were carried out on individual *P. trichocarpa* trees transferred from the greenhouse to the laboratory. $^{13}\text{C}_2$ -acetate delivery to leaves was accomplished using detached branches ($N = 3$ branches, 1 branch/individual) placed in a 10 mM solution of sodium $^{13}\text{C}_2$ -acetate (Sigma-Aldrich) for 2 days inside an environmentally controlled growth chamber (Percival Intellus Control System) maintained at 27.5°C daytime temperature (6:00–20:00; 30% light) and 23°C nighttime temperature (20:00–6:00). After 2 days, the branches took up roughly 30–40 ml of the $^{13}\text{C}_2$ -acetate solution. In addition, a single individual of 2.1 m height was placed in the laboratory under automated daytime lighting with continuous daytime (150 $\mu\text{l min}^{-1}$) and nighttime (70 $\mu\text{l min}^{-1}$) xylem injection at the base of the stem with a 10 mM sodium $^{13}\text{C}_2$ -acetate solution (1176 ml injected over 7 days using a flow controlled M6 Pump, Valco Instruments Co. Inc). Following the $^{13}\text{C}_2$ -acetate labelling period (branch: 2-day, tree: 7-day), a mature leaf was removed and flash frozen under liquid nitrogen and stored at -80°C before isolating whole leaf cell walls through the generation of AIR. Leaf AIR samples were also prepared from detached branches fed with water and 10 mM acetate with natural $^{13}\text{C}/^{12}\text{C}$ abundance as controls. Experimental details of the AIR saponification followed by ^{13}C -labelling analysis of the released acetate can be found in the supplementary methods.

3 | RESULTS

3.1 | Leaf gas exchange and water potential responses to experimental drought

Following the cessation of soil moisture additions on Day 0, large impacts on leaf water use and CO_2 metabolism could already be observed by Day 1 of the drought (Figure 1). For example, mean stomatal conductance (g_s) values of drought treated plants declined from 1.1 $\text{mol m}^{-2} \text{s}^{-1}$ on Day 0 to 0.026 $\text{mol m}^{-2} \text{s}^{-1}$, representing a 97% decrease. These low conductance values were maintained throughout the drought treatment on Day 4 and 7. As expected from a strong drought-induced decrease in g_s , leaf gas exchange of CO_2 and H_2O in the light showed a large suppression in drought-treated plants. Under standard environmental conditions, average net photosynthesis (A) decreased from 13.4 $\mu\text{mol m}^{-2} \text{s}^{-1}$ on Day 0 to $-0.5 \mu\text{mol m}^{-2} \text{s}^{-1}$ on Day 1, representing a 104% decrease and loss of net carbon assimilation. These near zero and often negative net CO_2 assimilation values continued in the drought plants through Days 4 and 7. Likewise, leaf transpiration (E) decreased by 94% on Day 1 as a result of the experimental drought treatment with average

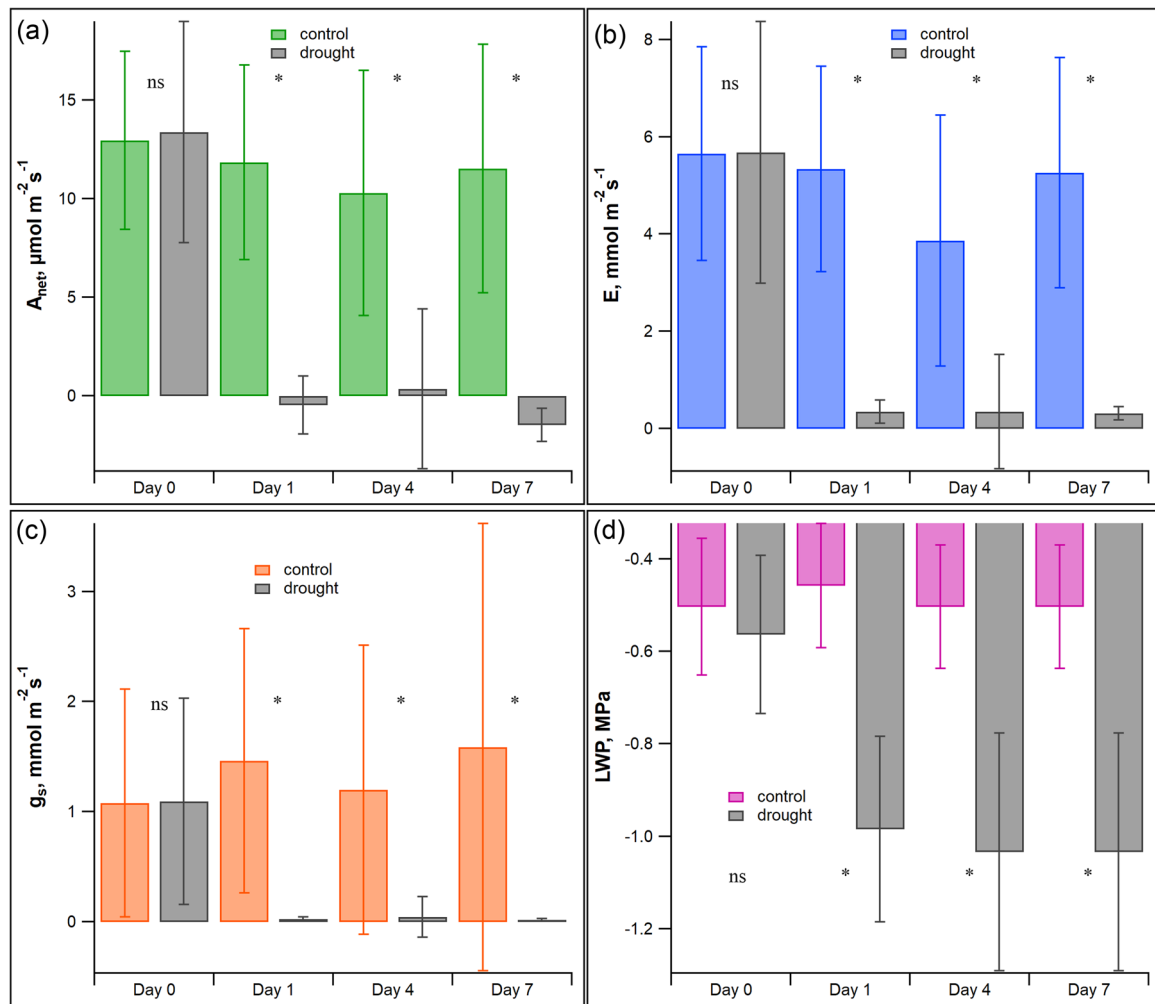


FIGURE 1 Leaf physiological parameters in control and drought treated plants. Poplar saplings were subject to drought for 7 days. Leaf observations were made on Day 0 ($n = 24$), Day 1 ($n = 6$), Day 4 ($n = 18$) and Day 7 ($n = 18$) of (a) Net photosynthesis (A_{net} , $\mu\text{mol m}^{-2} \text{s}^{-1}$), (b) transpiration (E , $\text{mmol m}^{-2} \text{s}^{-1}$), (c) stomatal conductance (g_s , $\text{mmol m}^{-2} \text{s}^{-1}$) and (d) leaf water potential (LWP, MPa). Values are plotted as average \pm 1 standard deviation (ns indicates no statistical significance between control and drought treatments, * indicates statistically significant difference, $p < 0.05$).

values declining from $5.7 \text{ mmol m}^{-2} \text{s}^{-1}$ on Day 0 to $0.33 \text{ mmol m}^{-2} \text{s}^{-1}$ on Day 1. These low leaf transpiration values continued through Days 4 and 7. The strong reduction in g_s , A , and E observed during on Days 1, 4 and 7 in drought-treated individuals was associated with a decrease in leaf water potential (LWP). Average LWP declined from -0.56 MPa in drought-treated leaves on Day 0 to -1.0 on Days 1, 4 and 7, representing a 79% decline. After the drought treatment, despite daily soil moisture additions resuming for the droughted trees, all the trees lost their leaves.

3.2 | Branch MeOH and AA emission responses to experimental drought

During the drought experiment, a subset of drought ($N = 6$) and control ($N = 6$) plants were transported to the analytical laboratory in the morning and analyzed for 'snap-shot' branch MeOH and AA

emissions for 1 h in a constant light and temperature environment (Figure 2a–c). Control plants had high average rates of MeOH emissions ($2.3\text{--}4.4 \text{ nmol m}^{-2} \text{s}^{-1}$) and low, but detectable levels of AA emissions ($0.1 \text{ nmol m}^{-2} \text{s}^{-1}$). In contrast, drought-stressed trees showed low MeOH emissions ($0.3 \text{ nmol m}^{-2} \text{s}^{-1}$) while also showing higher average AA emissions ($0.2 \text{ nmol m}^{-2} \text{s}^{-1}$). This pattern resulted in lower branch 'snap-shot' AA/MeOH emission ratios for the control plants ($10\% \pm 10\%$) relative to drought stressed plants ($84\% \pm 57\%$).

In contrast to greenhouse drought experiments which showed rapid negative leaf physiological effects, a second set of drought experiments occurred in a cooler lab, where artificial lighting was provided and gas exchange fluxes from a canopy branch were continuously monitored. While variability in the timing and magnitudes of the MeOH and AA emissions was observed between the five individuals, the same general emission pattern was observed during the real-time emission studies as those from the 'snap-shot' studies with drought inducing a pattern of decreasing branch MeOH

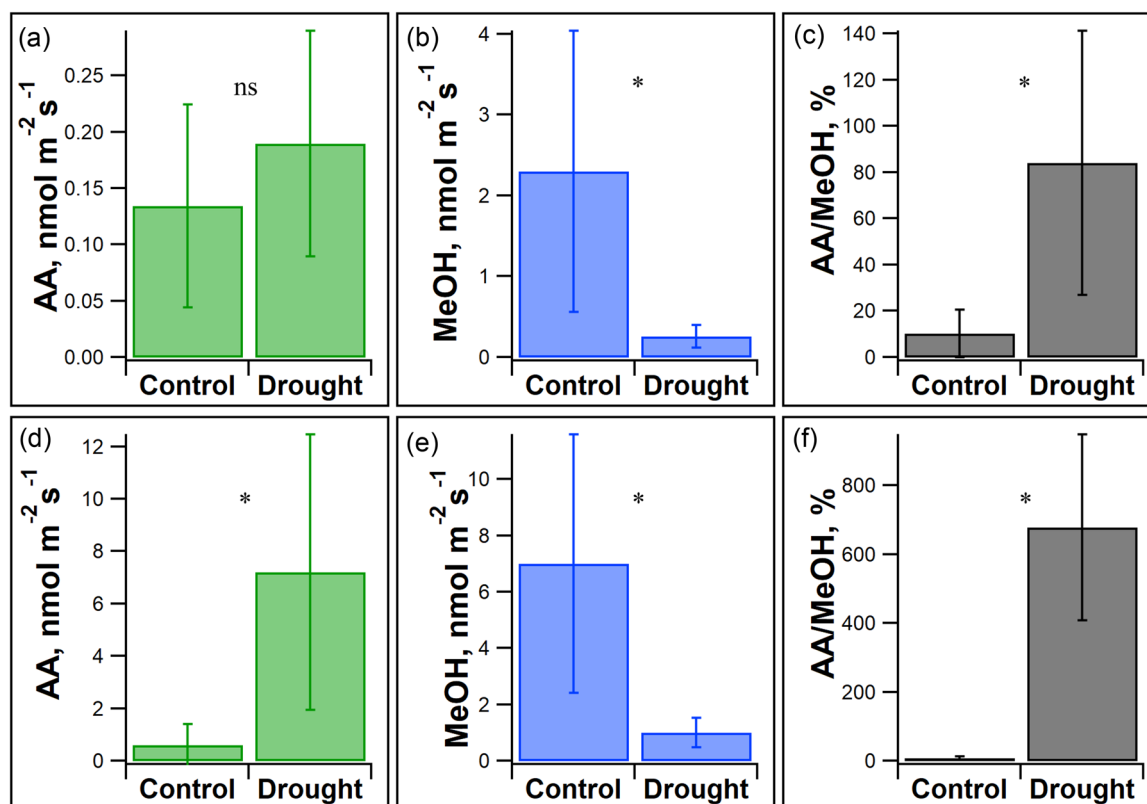


FIGURE 2 Branch daytime 'snap-shot' branch emissions of (a) acetic acid (AA), (b) methanol (MeOH), and (c) the AA/MeOH emission ratio from control ($N = 21$) and drought stressed ($N = 16$) poplar trees measured on Day 1 of the drought. In addition, the daily maximum (d) AA emissions, (e) MeOH emissions, and (f) AA/MeOH emission ratios from real-time branch gas exchange measurements on the first day of secession of soil water addition (Day 0: control) and a subsequent day during the drought response at the time where AA emissions were maximized ($N = 5$) are also shown. All values are plotted as average \pm one standard deviation (ns indicates no statistical significance between control and drought treatments, * indicates statistically significant differences, $p < 0.05$). [Color figure can be viewed at wileyonlinelibrary.com]

emissions and increasing AA emissions together with high AA/MeOH emissions ratios (Figures 2d–f and 3 and Supporting Information: Figures S2–5).

When the temporal patterns of branch gas exchange during drought was analyzed in more detail, four distinct phases could be described. The first 'growth phase' with physiologically active foliage is characterized by high rates of transpiration, net photosynthesis, and MeOH emissions, with low AA emissions. High MeOH emissions relative to AA emissions from physiologically active branches in the 'growth phase' constrain daytime AA/MeOH emission ratios to low values, reaching maximum mid-day values of 6% (e.g., Day 3 in Figure 3). The second phase of drought response consists of a strong suppression in MeOH emissions, apparently occurring before any reductions in stomatal conductance and CO₂ and H₂O gas exchange (e.g., Day 4). Although AA emissions remained low, branch AA/MeOH emission ratios during this 'MeOH suppression' phase increased slightly from 18% on Day 4 to 24% on Day 5. The third phase of drought response is characterized by a reduction in transpiration and net photosynthesis rates, a continued strong suppression of MeOH emissions, together with high branch emissions of the fermentation volatiles acetaldehyde, ethanol, acetic acid (AA), and acetone (e.g., initiated on Day 5 in Figure 3). High rates of fermentation VOC emissions were found to be initiated both during the day and the

night, depending on the individual (Supporting Information: Figures S2–S5). Emissions of acetaldehyde during this 'fermentation phase' were far higher than those of the other fermentation VOCs whose emissions generally tracked acetaldehyde. Elevated branch fermentation VOC emissions continued for 3 days, with the peak in AA/MeOH emission ratio (444%) occurring on Day 6. Throughout this 'fermentation phase', daytime transpiration and net photosynthesis continued to decline. During the final 'senescence phase' (Day 7–10), likely associated with irreversible damage to cellular components including photosynthetic membranes, isoprene emissions were suppressed, while AA/MeOH emission ratios declined, remaining high and reaching a value of 50% by Day 10.

To test for the potential reversibility of the suppression of branch MeOH emission during drought, when a drought-stressed potted tree showed strong suppression of MeOH emissions in the laboratory, re-watering of the soil with 100 ml additions on Day 4 (red arrows in Supporting Information: Figure S6), resulted in a rapid (~15 min) return of high branch MeOH emissions and a dramatic reduction of the AA/MeOH emission ratios to around 1%. As the soil continued to dry through the experiment, the suppression of MeOH emissions was again rapidly relieved by a 100 ml soil moisture addition, regardless of whether it was added during the day or night.

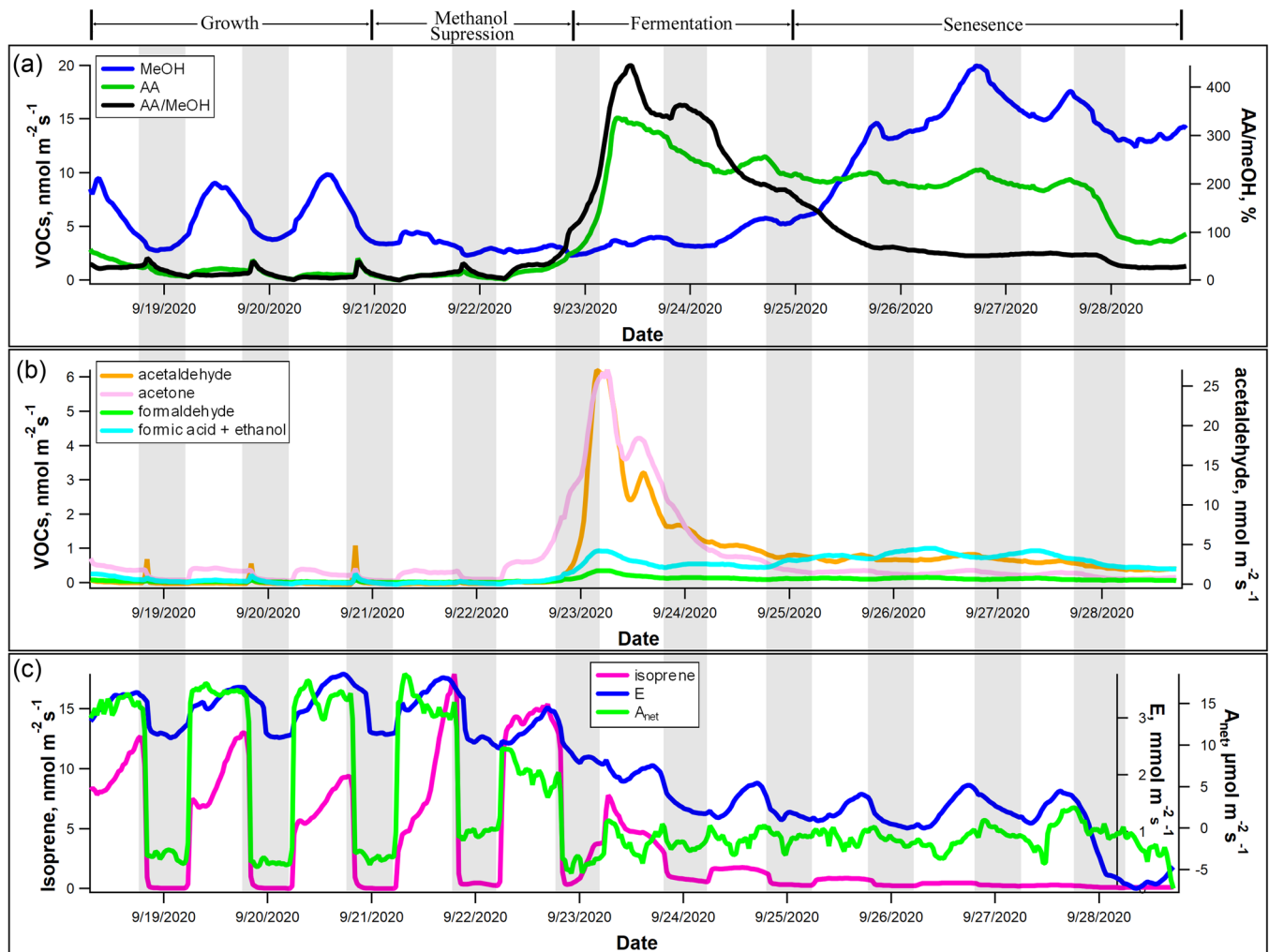


FIGURE 3 Real-time branch emissions of VOCs together with transpiration (E , $\text{mmol m}^{-2} \text{s}^{-1}$) and net photosynthesis (A_{net} , $\mu\text{mol m}^{-2} \text{s}^{-1}$) fluxes during a 10-day drought experiment. A branch enclosure was installed on a potted poplar tree and water withheld for the 10-day duration. Daily branch flux patterns of (a) Methanol (MeOH), Acetic Acid (AA), AA/MeOH emission ratio, (b) Aerobic fermentation intermediates (acetaldehyde, ethanol, acetone) (c) CO_2 and H_2O and the photosynthetic product isoprene. Shaded areas represent the night-time where the grow light was switched off. [Color figure can be viewed at wileyonlinelibrary.com]

This effect of water addition on droughted plants, completely altered the normal diurnal cycle in MeOH emissions which normally peak around mid-day in well-watered individuals. Maximum AA/MeOH emission ratios were 12% which were lower than those from branches of the five trees for which water was completely withheld (Figure 3 and Supporting Information: Figures S2–5) which showed high maximum AA/MeOH emission ratios ranging from 400% to 3500%.

3.3 | Leaf MeOH and AA emission responses to CO_2 , light and temperature

In order to evaluate the effect of environmental conditions on well hydrated poplar branches at the leaf level, MeOH and AA emissions, AA/MeOH ratio, stomatal conductance (g_s), transpiration, and net photosynthesis (P_{net}) measurements occurred in parallel during CO_2 , light, and

temperature leaf response studies. To minimize leaf water stress, poplar branches were detached, recut under water, with the target leaf placed in the chamber and the rest of the branch placed in a hydrated atmosphere in the dark. In this way, leaf hydration was maximized by shutting down transpiration from all leaves on the branch except the leaf inside the dynamic leaf chamber. Across the CO_2 ($A_{\text{net}}-C_i$, Figure 4a–c), light ($A_{\text{net}}-\text{PAR}$, Figure 4d–f) and temperature ($A_{\text{net}}-\text{leaf temp.}$, Figure 4g–i) response curves, MeOH and AA emissions generally tracked patterns of g_s and E , and did not appear to be strongly dependent on A_{net} . During the C_i response curves, MeOH emissions tended to increase at low C_i and decrease at high C_i , together with g_s . During the light curves, g_s values remained high and increased only slightly as a function of PAR, while MeOH and AA emissions also remained relatively stable. In contrast, as leaf temperature increased, g_s declined considerably at high leaf temperature (e.g., above 35°C), while MeOH and AA emissions together with transpiration generally increased up to the highest leaf temperatures (40°C). While g_s continued to decline in the dark at 40°C ,

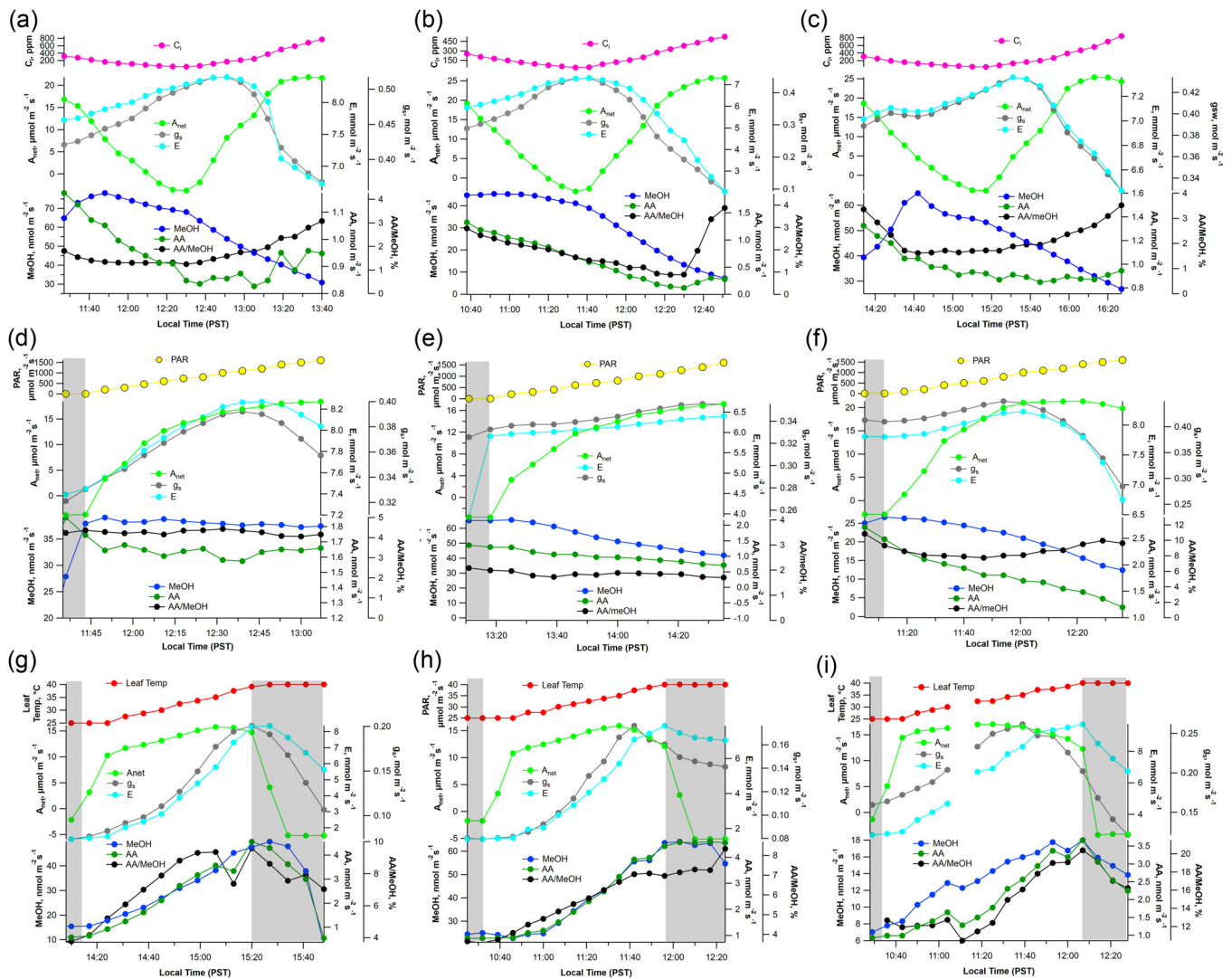


FIGURE 4 Dynamic leaf gas exchange responses of methanol, acetic acid, AA/MeOH, net photosynthesis (A_{net}), transpiration (E), and stomatal conductance (g_s) from detached hydrated poplar branches as a function of (a–c) leaf internal CO_2 concentrations (C_i), (d–f) incident Photosynthetically Active Radiation flux, and (g–i) leaf temperature. Shaded regions indicate dark conditions inside the leaf chamber. [Color figure can be viewed at wileyonlinelibrary.com]

leaf dark respiration caused A_{net} to quickly drop to negative values. In contrast, MeOH and AA emissions did not show a fast decline in the dark, but rather declined more gradually together with g_s and E . Importantly across C_i and PAR response curves, leaf AA/MeOH emission ratios remained relatively stable with maximum values <10%. In contrast, AA/MeOH emission ratios increased slightly as a function of temperature reaching maximum values in the light at 40°C of 10%–20%.

3.4 | Temperature sensitivities of MeOH and AA emissions and AA/MeOH emission ratios from physiologically active trees, detached stems and leaves, hydrated AIR and whole ecosystems

To better understand the role of temperature in enhancing AA/MeOH emission ratios, the sensitivity of MeOH and AA production

to air temperature was characterized using branches of well-watered poplar trees, detached stems and leaves, and whole ecosystems. Well-watered poplar trees were individually placed in a growth chamber with diurnally changing air temperature (Figure 5). At night in the dark (20:00–6:00), considerable branch transpiration was observed together with relatively high MeOH emissions, and low to undetectable AA emissions. Under constant daytime (6:00–20:00) light conditions, net positive CO_2 assimilation occurred. As observed at the leaf level, branch transpiration together with MeOH and AA emissions were strongly coupled to the diurnal pattern of air temperature, reaching maximum fluxes during the early afternoon peak in air temperature of 27°C at 14:00. MeOH emissions were greater than AA emissions at all air temperatures by roughly a factor of 10, except for 1 h following light to dark transitions where a short burst in AA emissions were observed. Outside of this light-dark period, branch AA/MeOH emission ratios remained low and

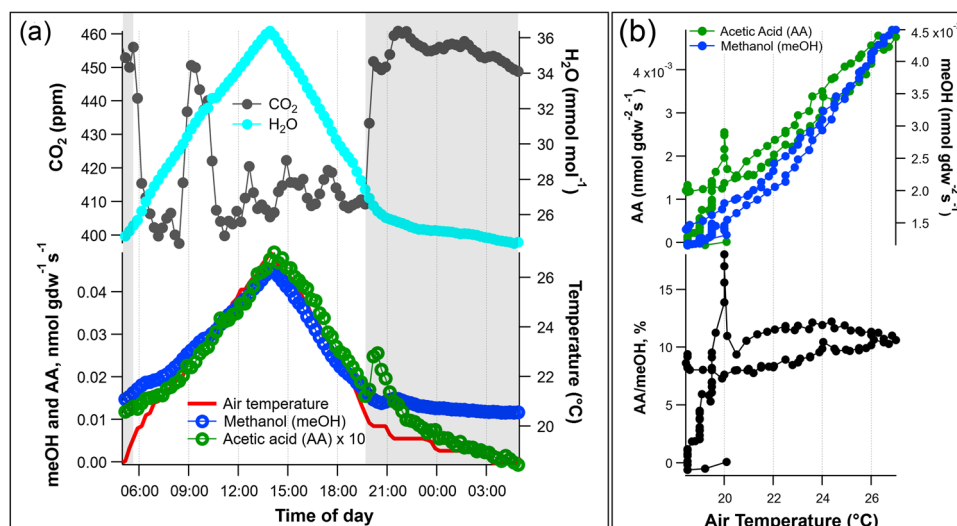


FIGURE 5 (a) Example diurnal pattern of acetic acid (AA) and methanol (MeOH) emissions from a physiologically active poplar branch from a tree inside a growth chamber programmed with a temperature increase during the day under constant illumination. (b) Also shown are AA and MeOH emissions and the ratio of AA/MeOH emissions plotted as a function of air temperature. Shaded areas represent the high-time where the grow light was switched off. [Color figure can be viewed at wileyonlinelibrary.com]

increased with air temperature up to ~12% (Figure 5). High temperature sensitivity of MeOH and AA emissions from detached poplar stem segments in the dark was also observed (Supporting Information: Figure S7). Similar temperature sensitivities of MeOH and AA emissions were also obtained from hydrated whole leaf cell wall preparations (alcohol insoluble residue, AIR). Gas-exchange analysis under controlled temperature with hydrated AIR in porous Teflon tubes showed rapid equilibration of MeOH and AA emissions within 10 min of reaching the new chamber temperature in the dark. MeOH and AA steady state emissions from hydrated AIR samples increased as a function of temperature from 30°C to 50°C (Figure 6) and were completely dependent on the presence of liquid water interacting with AIR (data not shown). Similar to physiologically active leaves (Figure 4), branches (Figure 5), and detached stems (Supporting Information: Figure S7), emissions from hydrated AIR were dominated by MeOH with AA/MeOH emission ratios increasing slightly with temperature but remaining below 30%.

In contrast, AA/MeOH emission ratios from drought stressed poplar branches reached high values ranging from 400 to 3000% (Figures 2–3, Supporting Information: Figures S2–S5). Similarly, detached poplar leaves placed into the temperature-controlled chamber in the dark in a dry air stream, showed a similar pattern of suppressed MeOH emissions together with temperature stimulated emissions of the fermentation volatiles acetaldehyde, ethanol, acetic acid, and acetone (Figure 7). Acetaldehyde emissions peaked at 42.5°C, AA emissions peaked at 47.5°C, and the AA/MeOH emission ratio reached a maximum of 2500% at 45°C.

When this analysis was applied to previously published datasets at the ecosystem scale during the growing season, average ecosystem emission rates of AA and MeOH (Belgium) and ambient concentrations (Belgium, Alabama, and California) showed clear diurnal patterns closely tracking air temperature. Moreover, ecosystem AA/MeOH emission and

concentration ratios increased linearly as a function of air temperature, peaking in the afternoon (Supporting Information: Figures S8–9). The diurnal increase in MeOH/AA concentration ratios in California and Alabama remained below 30%, suggesting that drought conditions were not experienced by the ecosystems.

3.5 | Changes in cell wall composition and esterification patterns in response to drought stress

In order to investigate the potential source(s) of MeOH and AA emissions from poplar leaves and evaluate potential impacts of drought stress on the cell wall polysaccharide composition, leaf bulk monosaccharide composition was determined from AIR samples. Consistent with the expected high pectin content of rapidly expanding leaf primary cell walls, monosaccharide content of AIR from poplar leaves was dominated by galacturonic acid (GalA, Figure 8a). While the monosaccharide content, and by extension polysaccharide content of the cell walls remained largely unchanged during drought, we observed an increase in O-acetyl ester content during drought (Figure 8b). AIR from control leaves released an average of 0.69 $\mu\text{g g}^{-1}$ of free acetate following saponification which increased by 10% to 0.76 $\mu\text{g g}^{-1}$ of free acetate g^{-1} from drought stressed leaves. Leaf AIR O-acetyl ester content increased throughout the drought, reaching a maximum after 7 days (Figure 8b).

3.6 | Evaluating acetate in the transpiration stream as a substrate for cell wall O-acetylation

To evaluate potential mechanisms involving rapid changes in cell wall O-acetylation in response to drought stress, experiments

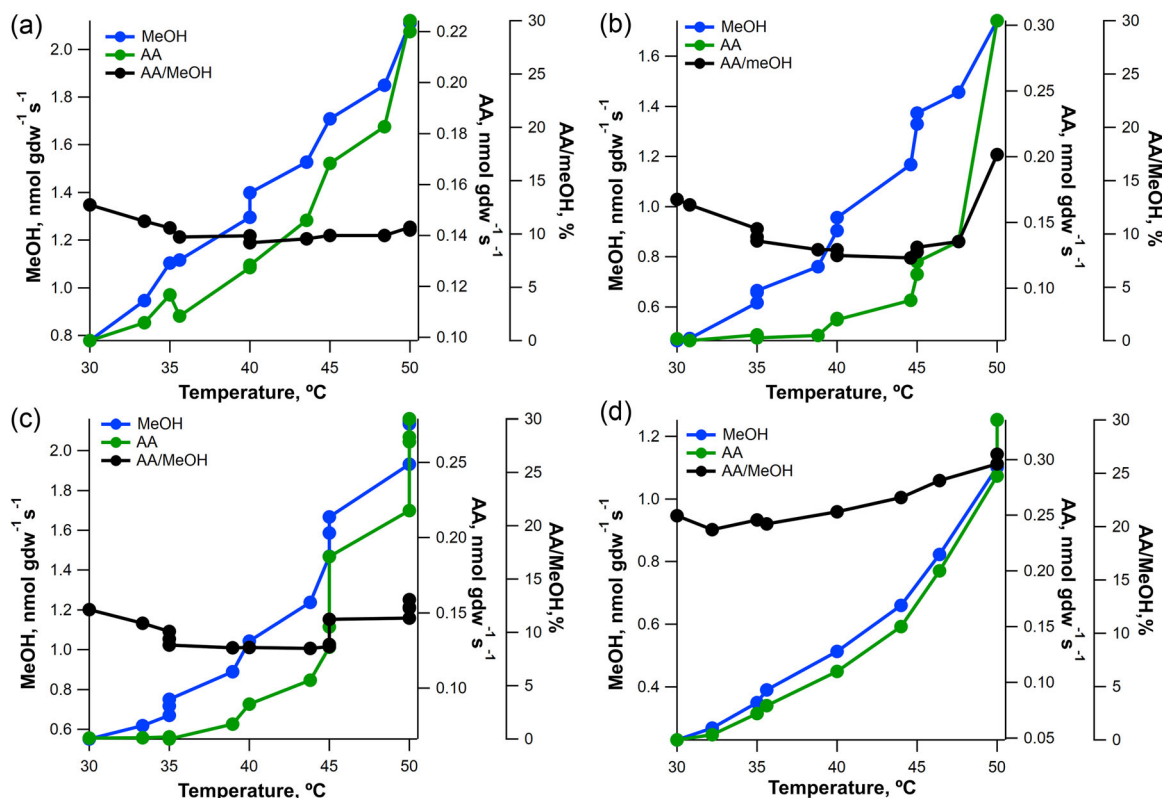


FIGURE 6 Emissions of methanol (MeOH) and acetic acid (AA) as a function of time from hydrated leaf cell wall isolates (AIR) in porous Teflon PTFE diffusion tubes as chamber air temperature increased from 30°C to 50°C. [Color figure can be viewed at wileyonlinelibrary.com]

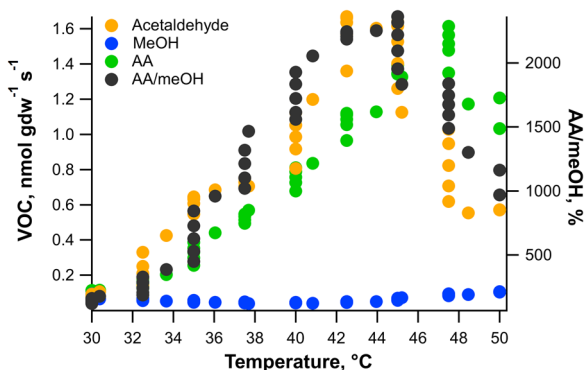


FIGURE 7 Example Acetaldehyde and Acetic Acid (AA) emissions from a detached poplar leaf in the dark with 1.0 L min dry air passing over in a temperature-controlled chamber (Ethanol and Acetone emissions are not shown for clarity). Average Acetaldehyde, AA, MeOH, and AA/MeOH emission values are plotted at each chamber temperature. [Color figure can be viewed at wileyonlinelibrary.com]

investigating the transport of doubly ^{13}C -labelled $^{13}\text{C}_2$ -acetate in the transpiration stream of detached branches and a whole intact tree were carried out. To evaluate leaf cell wall *O*-acetylation responses to $^{13}\text{C}_2$ -acetate in the transpiration stream, cell wall preparations (AIR) were isolated from canopy leaves, and saponified with deuterated sodium hydroxide (NaOD) to quantitatively hydrolyse the esters. The

resulting solution was analyzed for acetate isotopologues including monoisotopic acetate ($^{12}\text{C}_2$ -acetate) and acetate with one (^{13}C -1-acetate, ^{13}C -2-acetate), and two- ^{13}C -atoms ($^{13}\text{C}_2$ -acetate), by one-dimensional ^1H -NMR (Figure 9).

Acetate released upon saponification of the AIR (from 10 mg dried AIR/mL 0.4 M NaOD) ranged in concentration between 212 and 333 nmol/mg AIR (dry wt.), corresponding to 2.12 mM and 3.33 mM. The concentration of acetate in the method blank was 0.006 mM and, to quantify any additional free acetate that may have been present, incubations of AIR in only D_2O were also carried out. Free acetate was only quantifiable in two detached branch leaf samples at (1.2 and 1.4 nmol/mg AIR (dry wt.), or 0.012 and 0.014 mM. In the two cases where it was quantifiable, the highest amount of free acetate in the AIR amounted to less than 0.7% of the total concentration of acetate observed after saponification with 0.4 M NaOD.

The isotopologue distributions were determined from the experimental spectra (Figure 9) by integrating the peak areas corresponding to each isotopologue and dividing by the sum of the integrated areas of all acetate peaks. The results are summarized in Table 1 as the fraction of isotopologue divided by its expected fraction at natural abundance wherein a value of 1 indicates no change. In leaf cell AIR, there was an increase in the $^{13}\text{C}_2$ -acetate isotopologue by a factor of 125 ± 31 above its expected fraction at natural abundance along with concomitant

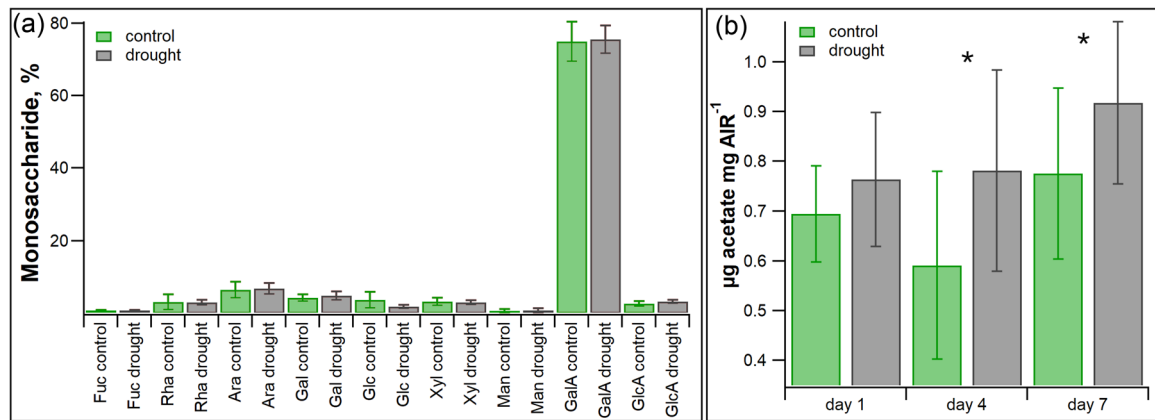
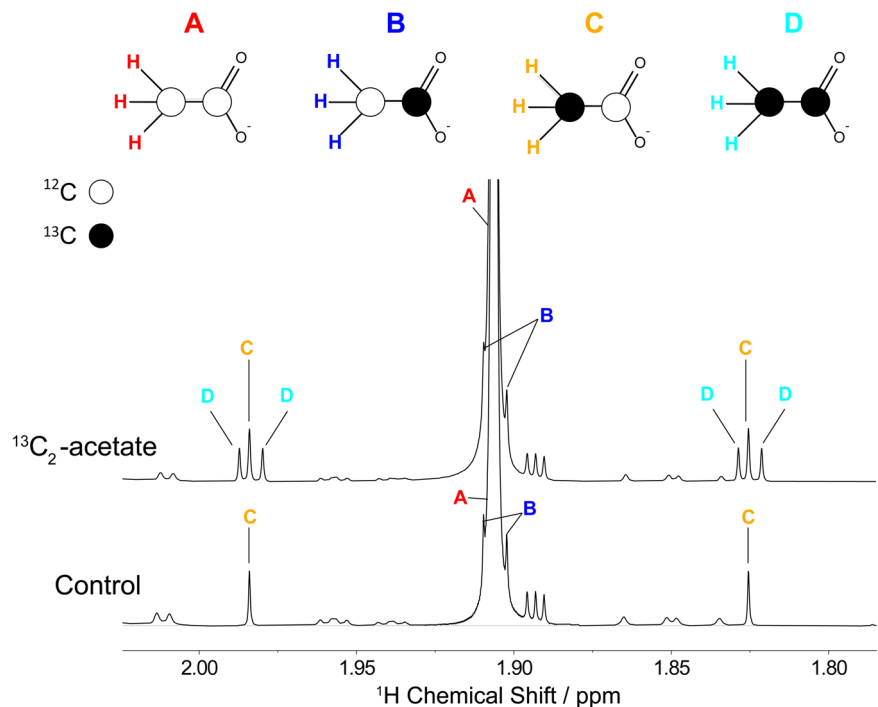


FIGURE 8 (a) Leaf bulk cell wall monosaccharide composition from control and drought stressed poplar trees one day following cessation of soil moisture additions. Monosaccharides quantified are fucose (Fuc), rhamnose (Rha), arabinose (Ara), galactose (Gal), glucose (Glc), xylose (Xyl), mannose (Man), galacturonic acid (GalA) and glucuronic acid (GlcA). (b) Also shown are leaf bulk cell wall O-acetyl methyl ester content released following saponification of alcohol insoluble residue (AIR) preparations from control and drought stressed leaves on day 1, 4 and 7. Values are plotted as average \pm one standard deviation (* indicates statistically significant difference between control and drought treatments, $p < 0.05$). Note, no statistically significant differences were observed in monosaccharide composition between control and drought treatments during Days 1, 4 or 7. [Color figure can be viewed at wileyonlinelibrary.com]

FIGURE 9 Exploring the mechanism of leaf bulk cell wall O-acetylation. Simplified schematic showing acetate and its four-stable carbon isotopologues with 0 (A), 1 (B and C) and 2 (D) ^{13}C atoms. Following delivery of a 10 mM $^{13}\text{C}_2$ -acetate to detached poplar branches and a whole poplar tree via the transpiration stream, leaf cell walls were isolated and analyzed by ^1H -NMR. Note: the much more intense $^{12}\text{C}_2$ -isotopologue signal (A) was clipped vertically in both control and $^{13}\text{C}_2$ -acetate spectra to show the details of the satellite peaks corresponding to the remaining isotopologues which are labelled B–D. The acetate $^1J_{\text{CH}} = 127.0 \pm 0.1$ Hz and the $^2J_{\text{CH}} = 5.9 \pm 0.1$ Hz. [Color figure can be viewed at wileyonlinelibrary.com]



decreases in the fractions corresponding to the remaining isotopologues. For example, no significant changes or slight decreases were detected in the relative abundances of mono-labelled ^{13}C -1-acetate and ^{13}C -2-acetate isotopologues. An increase in the fraction of $^{13}\text{C}_2$ -acetate isotopologue by a factor of 48 ± 7 was also observed in two of the three canopy leaf samples collected following 1 week of 10 mM $^{13}\text{C}_2$ -acetate solution continuously injected into the xylem of an intact potted tree.

During branch and whole tree labelling with $^{13}\text{C}_2$ -acetate, plant emission data was collected for three different isotopologues of acetic acid in real-time using PTR-MS including $^{12}\text{C}_2$ -AA, ^{13}C -1-AA + ^{13}C -2-AA and $^{13}\text{C}_2$ -AA. During the whole tree labelling with $^{13}\text{C}_2$ -acetate via the transpiration stream, significant branch emissions of $^{13}\text{C}_2$ -AA were not observed. However, leaf emissions of $^{13}\text{C}_2$ -AA could be observed in some of the detached branch experiments (e.g., Supporting Information: Figure S8), confirming the delivery of the labelled acetate to the leaves.

TABLE 1 ^1H -NMR isotopologue analysis results for acetate released following saponification of isolated leaf cell wall samples from (a) 3 detached branches (one per tree, $N = 3$) treated with 10 mM $^{13}\text{C}_2$ -acetate solution for 2 days as well as (b) canopy leaf ($N = 3$) samples from a 2-year old tree following continuous diurnal injections of the 10 mM $^{13}\text{C}_2$ -solution into the xylem at the base of the tree for 7 days (night: 70 $\mu\text{l}/\text{min}$, day: 150 $\mu\text{l}/\text{min}$).

Leaf sample	Acetate isotopologue	$F_{\text{experiment}}/F_{\text{natural abundance}}$
Detached branch	$^{12}\text{C}_2$ -acetate	0.985 ± 0.008 (*)
Detached branch	^{13}C -1-acetate	0.6 ± 0.3 (ns)
Detached branch	^{13}C -2-acetate	1.00 ± 0.09 (ns)
Detached branch	$^{13}\text{C}_2$ -acetate	125 ± 31 (*)
Whole tree	$^{12}\text{C}_2$ -acetate	0.995 ± 0.004 (ns)
Whole tree	^{13}C -1-acetate	0.9 ± 0.2 (ns)
Whole tree	^{13}C -2-acetate	1.01 ± 0.04 (ns)
Whole tree	$^{13}\text{C}_2$ -acetate	48 ± 7 (*)

Note: Following saponification of the cell wall isolates, the values were obtained by integrating the area of the free acetate signals (corresponding to each of the four isotopologues shown in Figure 10), and calculating the fraction of each acetate isotopologue to the total ($F_{\text{experiment}} = \text{peak area acetate isotopologue}/\text{peak area of total acetate isotopologues}$), and reporting the ratio of F_{exp} to that from natural abundance fractions ($F_{\text{natural abundance}}$). Note, statistically significant changes in $F_{\text{experiment}}/F_{\text{natural abundance}}$ (*), no statistically significant changes (ns).

4 | DISCUSSION

4.1 | Pectin, methanol and the growing plant cell wall

The polysaccharide pectin can account for up to 35% of the primary cell wall in dicots and nongrass monocots, and up to 5% of wood tissues (Mohnen, 2008). Newly synthesized pectin in the primary cell wall is known to be highly methyl esterified, with changes in the degree of pectin methylesterification mediated by pectin methyl esterases (PME) known to regulate cell wall mechanical properties like elasticity. The degree of pectin methylesterification can have profound impact on physiological processes like tissue morphogenesis and growth as well as numerous biological functions (Levesque-Tremblay et al., 2015). Cell wall synthesis is coupled to changes in cell wall elasticity mediated by pectate formation following pectin demethylesterification (Peaucelle et al., 2012). In *Arabidopsis*, increases in tissue elasticity in living meristems correlated with pectin demethylesterification (Peaucelle et al., 2011) which is required for the initiation of organ formation (Peaucelle et al., 2008). When pectin demethylation was inhibited, stiffening of the cell walls throughout the meristem was observed which completely blocked

the formation of primordia (Peaucelle et al., 2008). Thus, pectin demethylation is a critical process that regulates the direction and speed of cell wall expansion during growth and morphogenesis (Braybrook et al., 2012). Consistent with the view that MeOH emissions from plants into the atmosphere primarily derive from pectin demethylation, numerous studies have revealed that leaf methanol emissions tightly correlate with leaf expansion rates (Hüve et al., 2007) with young rapidly expanding leaves emitting higher fluxes of MeOH than mature leaves (Jardine et al., 2016). Our temperature-controlled gas exchange observations of hydrated leaf bulk cell walls (AIR) provide new direct evidence for pectin demethylation as the dominant source of foliar MeOH emissions. The observations suggest that in addition to enzymatic hydrolysis reactions catalysed by esterase enzymes within the cell wall, temperature stimulated nonenzymatic hydrolysis of cell wall methyl and *O*-acetyl esters may be an important source of MeOH and AA production in situ. Purified whole leaf cell walls (AIR) hydrated and placed in a porous Teflon tubes permitting gas exchange showed remarkably similar temperature sensitivities of MeOH and AA emissions (Figure 6) as physiologically active leaves (Figure 4), branches (Figure 5), detached stems (Supporting Information: Figure S7), and whole ecosystems (Supporting Information: Figures S8–9), confirming plant cell walls as an important source of MeOH and AA emissions.

In contrast to growth processes, abiotic stress responses may be associated with increased cell wall fortification through a reduction in pectin demethylation rates mediated by pectin methyl esterase inhibitors (PMEI). For example, abiotic stress may lead to the inhibition of pectin demethylation via enhanced expression of PMEI genes known to be involved in abiotic stress tolerance (An et al., 2008; Hong et al., 2010; Ren et al., 2019; Wang et al., 2020). Recent work on drought response of leaf-succulent *Aloe vera* reported the drought-induced folding of hydrenchyma cell walls involves changes in pectin esterification (Ahl et al., 2019). It was hypothesized that the cell wall folding process during drought may be initiated by a reduction in pectin de-esterification and its associated MeOH production and Ca^{+2} -complexation, thereby releasing internal constraints on the cell wall. Thus, we suggest that the strong decrease in observed foliar MeOH emissions during water stress (Figures 2,3,7, Supporting Information: S2–5) may be related to both g_s reductions and reduced cell wall de-methylation rates related to increased PMEI activity. We speculate that reductions in tissue water potential leads to the inhibition of pectin methyl ester hydrolysis, MeOH production, and growth.

Results from the leaf-level environmental response curves (Figure 4) are consistent with the view that stomatal regulated leaf MeOH emissions are controlled by light-independent, but highly temperature-dependent production associated with growth processes (Harley et al., 2007). Thus, light and CO_2 are assumed to only indirectly influence leaf MeOH emission rates via changes to g_s . However, we highlight that reduction of g_s at high temperatures in well hydrated leaves was often unable to prevent the temperature increase in MeOH and AA emissions (Figure 4). Similarly, reductions

in g_s during drought were unable to suppress the emissions of fermentation volatiles like AA (Figures 2,3, Supporting Information: S2–5). Although a link with g_s is possible, our observations suggest that the large changes in AA/MeOH ratios during growth and drought stress responses are largely due to changes in production rates, with MeOH production declining and AA production increasing during different phases of the drought response (Figure 3). Our study suggests that there are at least two distinct plant sources of atmospheric AA emissions; hydrolysis of O-acetyl groups on the cell wall (Figure 6) and the aerobic fermentation pathway (Figures 3, 7). The metabolic origin of AA is further discussed in the Supporting Information.

4.2 | Cell wall O-acetylation is modified by drought

In this study, we found statistically significant enrichments in O-acetyl ester content of bulk leaf cell walls (AIR) in response to drought stress (Figure 8b). In contrast, cell wall monomer composition, which was dominated by galacturonic acid from pectin, changed little over 7 days following the cessation of watering (Figure 8a). That leaf AIR monosaccharide content was largely insensitive to drought suggests a slower turnover in monosaccharide cell wall polysaccharides than the fast time scales of days observed for changes in volatile emission signatures and cell wall O-acetyl ester content changes (1–7 days). O-acetyl-substituents are present on nearly all cell wall polymers with the exception of cellulose, whereas methyl esters are thought to be primarily associated with pectin (Derbyshire et al., 2007). O-acetyl esterification of plant cell walls is known to play important physicochemical, mechanical, and structural roles that serve to minimize degradation while enhancing intermolecular interactions with other wall polymers (Biely, 2012). Studies have shown that cell wall O-acetylation of hemicellulose and pectin is critical for proper plant growth and functioning. For example, simultaneous mutations of the acetyl transferase genes *TBL32*, *TBL33* and *TBL29/ESK1* in *Arabidopsis* resulted in a severe reduction in xylan O-acetyl level down to 15% that of the wild type, and concomitantly, severely collapsed vessels and stunted plant growth (Yuan et al., 2016). Likewise, strongly reduced growth and collapsed vessels were found in *Arabidopsis* mutated in the four Reduced Wall Acetylation genes, which may encode Golgi-localized transporters of substrates for acetyl transferases (Manabe et al., 2013). Additional studies demonstrated that *Arabidopsis* plants with defective *TBL29/ESK1* enzymes have a constitutive drought syndrome and collapsed xylem vessels, low hydraulic conductivity along with low O-acetylation levels in xylan and mannan, low transpiration rates, high water use efficiency, and dwarfism (Lefebvre et al., 2011; Ramírez et al., 2018). Together with these studies, the observation of enhanced leaf cell wall O-acetylation during drought (Figure 8b) suggests that polysaccharide O-acetylation is important for the proper functioning of vascular tissues under water deficit.

4.3 | Acetate as a potential substrate for cell wall O-acetylation

While the mechanisms of methyl esterification of pectin and its demethylation by PME have been the focus of several studies (Mohnen, 2008; Willats et al., 2001), the mechanisms of how O-acetyl groups are transferred to and from cell wall polymers and their role in the life cycle of a plant are poorly understood. Current biochemical models of cell wall esters assume that carbohydrate monomers are heavily O-acetylated using acetyl-CoA or another acetyl donor initially in the Golgi apparatus, and subsequently exported and incorporated into the growing cell wall. The wall polymers can then be de-esterified in the wall by esterase enzymes at a later point in the life cycle of the cell in support of numerous physiological and biochemical processes. Acetyl transfer activity from acetyl-CoA to xylooligomer acceptors has been attributed to Golgi localized TBL acetyl transferases (Urbanowicz et al., 2014; Zhong et al., 2017). Notably, acetyl donors such as *p*-nitrophenyl acetate and acetyl salicylic acid are even better substrates for TBL29 in vitro than acetyl-CoA (Lunin et al., 2020), and transport of acetyl CoA into the Golgi lumen has not been demonstrated. Hence, it is possible that the immediate donor for cell wall acetylation is not acetyl CoA but an unknown acetyl donor, although it may be generated from acetyl CoA. We observed that delivery of $^{13}\text{C}_2$ -acetate to the transpiration stream of poplar branches and xylem of a whole tree leads to rapid and significant $^{13}\text{C}_2$ -labelling of O-acetyl esters in isolated leaf cell walls (AIR). Therefore, activation of $^{13}\text{C}_2$ -acetate to $^{13}\text{C}_2$ -acetyl-CoA or an unidentified acetyl donor utilized by Golgi-localized acetyl transferases could explain the $^{13}\text{C}_2$ -labelling of O-acetyl esters observed in leaf cell walls isolations (AIR) (Table 1). $^1\text{H-NMR}$ analysis of the acetate released following leaf AIR saponification show that satellite signals corresponding to the $^{13}\text{C}_2$ -acetate isotopologue were detectable in all three detached branch leaf AIR samples and two of the three whole tree leaf AIR samples which had been treated with 10 mM $^{13}\text{C}_2$ -acetate via the transpiration stream. In contrast, AIR of leaves labelled with $^{13}\text{C}_2$ -acetate treated with water instead of NaOD did not show any detectable $^{13}\text{C}_2$ -acetate in solution, suggesting the acetate was bound to the cell wall material via an ester bond, making it unlikely that the delivered $^{13}\text{C}_2$ -acetate in the transpiration stream became trapped in the cell wall material, but not esterified.

These results suggest a possible link between the drought-induced increase in foliar AA emissions (e.g., Figure 3) and increased O-acetylation of leaf cell walls (Figure 8b). Thus, in addition to providing acetate for protein acetylation and defence gene regulation (Kim et al., 2017), the activation of aerobic fermentation during drought may also supply acetyl-CoA used in the Golgi prior to incorporation into the cell wall (Gou et al., 2012; Orfila et al., 2012; de Souza et al., 2014). This hypothesis is consistent with previous studies with microsomal preparations of a potato cell suspension culture that were supplied with ^{14}C -acetyl-CoA found radio-labelled acetate in an esterified form on several polysaccharides, including xyloglucan and pectin (Pauly & Scheller, 2000). Although the mechanisms require further investigation, our study is consistent

with cell wall methylation and O-acetylation of polysaccharides rapidly responding to environmental conditions, potentially allowing plants the flexibility to dynamically alter growth and defence processes. Our observations are consistent with a coordinated reduction in cell wall de-methyl esterification and growth processes during water stress (resulting in a strong suppression in MeOH production) together with an activation of defence processes including stomatal closure, aerobic fermentation (increasing AA production and emissions), and enhancements in cell wall O-acetylation.

4.4 | Conclusions and prospects

Although plants are known to activate growth suppression and defence signaling during abiotic stress, the biochemical, physiological, and ecological mechanisms involved are under intense investigation. In this study, we identified the active growth phase associated with rapid biomass accumulation and high rates of leaf gas exchange as highly enriched in MeOH emissions relative to AA. AA and MeOH emission patterns of hydrated leaf cell wall isolations (AIR) showed similar temperature sensitivities when compared with physiologically active poplar leaves, branches, and ecosystems. The striking similarities in temperature sensitivities of AA/MeOH emissions from AIR, leaves, branches, and whole ecosystems provides direct evidence for the cell wall as the main source of foliar MeOH and AA emissions during normal physiological activities. However, drought exposure led to large increases in AA/MeOH emissions (400%–3500%) linked to numerous coordinated leaf physiological and biochemical changes starting with a suppression of MeOH emissions followed by a suppression of net photosynthesis and transpiration, a large increase in foliar AA emissions, and increase in cell wall O-acetylation. While the metabolic origin of AA under drought stress requires further evaluation, we suggest that AA/MeOH emission ratios may be exploited by future plant and ecosystem studies as a highly sensitive atmospheric signal reflecting growth-defence trade-offs in plants and ecosystems as they move between optimal growth conditions and abiotic stress associated with decreased productivity.

ACKNOWLEDGEMENTS

This material is based upon work supported by the US Department of Energy (DOE), Office of Science, Office of Biological and Environmental Research (BER), Biological System Science Division (BSSD), Early Career Research Programme under Award number FP00007421 to Lawrence Berkeley National Laboratory. This work was also supported as part of the DOE Joint BioEnergy Institute through contract DE-AC02-05CH11231 to Lawrence Berkeley National Laboratory (LBNL). A portion of this research was performed on project awards (10.46936/cpcy. proj.2019.50708/60006566 and 10.46936/expl. proj.2019.51078/60006676) from the Environmental Molecular Sciences Laboratory, a DOE Office of Science User Facility sponsored by the BER programme under Contract No. DE-AC05-76RL01830. We would like to acknowledge extensive project

guidance from Eoin Brodie at (LBNL) and Christina Wistrom for the maintenance and establishment of our poplar trees at the UC Berkeley Oxford Greenhouse. In addition, we would like to acknowledge Thomas Powell for practical advice on leaf water potential measurements and the helpful discussions on cell wall elasticity and plant drought stress responses. Finally, we would like to express our sincere gratitude to PC&E associate editor Prof. Guillaume Tcherkez (Emeritus professor of Molecular Plant Physiology, Australian National University, Canberra) for his encouragement and extensive efforts to facilitate the review process which greatly improved the manuscript organization, readability, quantitative analysis, and conclusions on cell wall sources of MeOH and AA at high temperatures.

DATA AVAILABILITY STATEMENT

Data available on request from the authors.

ORCID

Kolby J. Jardine  <http://orcid.org/0000-0001-8491-9310>

Robert P. Young  <http://orcid.org/0000-0002-2686-9594>

Miguel Portillo-Estrada  <http://orcid.org/0000-0002-0348-7446>

REFERENCES

- Ahl, L.I., Mravec, J., Jørgensen, B., Rudall, P.J., Rønsted, N. & Grace, O.M. (2019) Dynamics of intracellular mannan and cell wall folding in the drought responses of succulent aloe species. *Plant, Cell & Environment*, 42, 2458–2471.
- Amsbury, S., Hunt, L., Elhaddad, N., Baillie, A., Lundgren, M., Verhertbruggen, Y. et al. (2016) Stomatal function requires pectin de-methyl-esterification of the guard cell wall. *Current Biology*, 26, 2899–2906.
- An, S.H., Sohn, K.H., Choi, H.W., Hwang, I.S., Lee, S.C. & Hwang, B.K. (2008) Pepper pectin methylesterase inhibitor protein CaPME1 is required for antifungal activity, basal disease resistance and abiotic stress tolerance. *Planta*, 228, 61–78.
- Aulia, M.R., Setiawan, Y. & Fatikhunnada, A. (2016) Drought detection of west java's paddy field using MODIS EVI satellite images (case study: rancaekek and rancaekek wetan). *Procedia Environmental Sciences*, 33, 646–653.
- Biely, P. (2012) Microbial carbohydrate esterases deacetylating plant polysaccharides. *Biotechnology Advances*, 30, 1575–1588.
- Braybrook, S.A., Hofte, H. & Peaucelle, A. (2012) Probing the mechanical contributions of the pectin matrix: insights for cell growth. *Plant Signaling & Behavior*, 7, 1037–1041.
- Chebli, Y. & Geitmann, A. (2017) Cellular growth in plants requires regulation of cell wall biochemistry. *Current Opinion in Cell Biology*, 44, 28–35.
- Derbyshire, P., McCann, M.C. & Roberts, K. (2007) Restricted cell elongation in Arabidopsis hypocotyls is associated with a reduced average pectin esterification level. *BMC Plant Biology*, 7, 31.
- Dewhirst, R.A., Afseth, C.A., Castanha, C., Mortimer, J.C. & Jardine, K.J. (2020) Cell wall O-acetyl and methyl esterification patterns of leaves reflected in atmospheric emission signatures of acetic acid and methanol. *PLoS One*, 15, e0227591.
- Dewhirst, R.A., Handakumbura, P., Clendinen, C.S., Arm, E., Tate, K., Wang, W. et al. (2021) High temperature acclimation of leaf gas exchange, photochemistry, and metabolomic profiles in *Populus trichocarpa*. *ACS Earth and Space Chemistry*, 5, 1813–1828.
- Dewhirst, R.A., Mortimer, J.C. & Jardine, K.J. (2020) Do cell wall esters facilitate forest response to climate? *Trends in Plant Science*, 25, 729–732.

- Fall, R. (2003) Abundant oxygenates in the atmosphere: a biochemical perspective. *Chemical Reviews*, 103, 4941–4952.
- Furtado, A., Lupoi, J.S., Hoang, N.V., Healey, A., Singh, S., Simmons, B.A. et al. (2014) Modifying plants for biofuel and biomaterial production. *Plant Biotechnology Journal*, 12, 1246–1258.
- Ganie, S.A. & Ahammed, G.J. (2021) Dynamics of cell wall structure and related genomic resources for drought tolerance in rice. *Plant Cell Reports*, 40, 437–459.
- Gille, S. & Pauly, M. (2012) O-acetylation of plant cell wall polysaccharides. *Frontiers in Plant Science*, 3, 12.
- Gou, J.-Y., Miller, L.M., Hou, G., Yu, X.-H., Chen, X.-Y. & Liu, C.-J. (2012) Acetyltransferase-mediated deacetylation of pectin impairs cell elongation, pollen germination, and plant reproduction. *The Plant Cell*, 24, 50–65.
- Harley, P., Greenberg, J., Niinemets, Ü. & Guenther, A. (2007) Environmental controls over methanol emission from leaves. *Biogeosciences*, 4(6), 1083–1099.
- Helm, L.T., Shi, H., Lerda, M.T. & Yang, X. (2020) Solar-induced chlorophyll fluorescence and short-term photosynthetic response to drought. *Ecological Applications*, 30, e02101.
- Hong, M.J., Kim, D.Y., Lee, T.G., Jeon, W.B. & Seo, Y.W. (2010) Functional characterization of pectin methyltransferase inhibitor (PMEI) in wheat. *Genes & Genetic Systems*, 85, 97–106.
- Hüve, K., Christ, M.M., Kleist, E., Uerlings, R., Niinemets, U., Walter, A. et al. (2007) Simultaneous growth and emission measurements demonstrate an interactive control of methanol release by leaf expansion and stomata. *Journal of Experimental Botany*, 58, 1783–1793.
- Jardine, K.J., Chambers, J.Q., Holm, J., Jardine, A.B., Fontes, C.G., Zorzanelli, R.F. et al. (2015) Green leaf volatile emissions during high temperature and drought stress in a central Amazon rainforest. *Plants*, 4, 678–690.
- Jardine, K.J., Fernandes de Souza, V., Oikawa, P., Higuchi, N., Bill, M., Porras, R. et al. (2017) Integration of C₁ and C₂ metabolism in trees. *International Journal of Molecular Sciences*, 18, 2045.
- Jardine, K.J., Jardine, A.B., Souza, V.F., Carneiro, V., Ceron, J.V., Gimenez, B.O. et al. (2016) Methanol and isoprene emissions from the fast-growing tropical pioneer species *Vismia guianensis* (Aubl.) Pers. (Hypericaceae) in the central Amazon forest. *Atmospheric Chemistry and Physics*, 16, 6441–6452.
- Ji, Y., Zhou, G., Li, Z., Wang, S., Zhou, H. & Song, X. (2020) Triggers of widespread dieback and mortality of poplar (*Populus* spp.) plantations across Northern China. *Journal of arid environments*, 174, 104076.
- Kim, J.-M., To, T.K., Matsui, A., Tanoi, K., Kobayashi, N.I., Matsuda, F. et al. (2017) Acetate-mediated novel survival strategy against drought in plants. *Nature Plants*, 3, 17097.
- Lefebvre, V., Fortabat, M.-N., Ducamp, A., North, H.M., Maia-Grondard, A., Trouverie, J. et al. (2011) ESKIMO1 disruption in *Arabidopsis* alters vascular tissue and impairs water transport. *PLoS One*, 6, e16645.
- Levesque-Tremblay, G., Pelloux, J., Braybrook, S.A. & Müller, K. (2015) Tuning of pectin methylesterification: consequences for cell wall biomechanics and development. *Planta*, 242, 791–811.
- Liu, Y., Zhou, R., Wen, Z., Khalifa, M., Zheng, C., Ren, H. et al. (2021) Assessing the impacts of drought on net primary productivity of global land biomes in different climate zones. *Ecological Indicators*, 130, 108146.
- Lunin, V.V., Wang, H.T., Bharadwaj, V.S., Alahuhta, M., Peña, M.J., Yang, J.Y. et al. (2020) Molecular mechanism of polysaccharide acetylation by the *Arabidopsis* xylan O-acetyltransferase XOAT1. *The Plant Cell*, 32, 2367–2382.
- Manabe, Y., Verhertbruggen, Y., Gille, S., Harholt, J., Chong, S.L., Pawar, P.M. et al. (2013) Reduced wall acetylation proteins play vital and distinct roles in cell wall O-acetylation in *Arabidopsis*. *Plant Physiology*, 163, 1107–1117.
- McDowell, N., Pockman, W.T., Allen, C.D., Breshears, D.D., Cobb, N., Kolb, T. et al. (2008) Mechanisms of plant survival and mortality during drought: why do some plants survive while others succumb to drought? *The New Phytologist*, 178, 719–739.
- Mohnen, D. (2008) Pectin structure and biosynthesis. *Current Opinion in Plant Biology*, 11, 266–277.
- Novaković, L., Guo, T., Bacic, A., Sampathkumar, A. & Johnson, K.L. (2018) Hitting the wall-sensing and signaling pathways involved in plant cell wall remodeling in response to abiotic stress. *Plants*, 7, 89.
- Orfila, C., Dal Degan, F., Jørgensen, B., Scheller, H.V., Ray, P.M. & Ulvskov, P. (2012) Expression of mung bean pectin acetyl esterase in potato tubers: effect on acetylation of cell wall polymers and tuber mechanical properties. *Planta*, 236, 185–196.
- Park, J.H., Goldstein, A.H. & Timkovsky, J. (2013) Eddy covariance emission and deposition flux measurements using proton transfer reaction–time of flight–mass spectrometry (PTR-TOF-MS): comparison with PTR-MS measured vertical gradients and fluxes. *Atmospheric Chemistry and Physics*, 13, 1439–1456.
- Pauly, M. & Keegstra, K. (2010) Plant cell wall polymers as precursors for biofuels. *Current Opinion in Plant Biology*, 13, 305–312.
- Pauly, M. & Scheller, H.V. (2000) O-Acetylation of plant cell wall polysaccharides: identification and partial characterization of a rhamnogalacturonan O-acetyl-transferase from potato suspension-cultured cells. *Planta*, 210, 659–667.
- Peaucelle, A., Braybrook, S. & Höfte, H. (2012) Cell wall mechanics and growth control in plants: the role of pectins revisited. *Frontiers in Plant Science*, 3, 121.
- Peaucelle, A., Braybrook, S.A., Le Guillou, L., Bron, E., Kuhlemeier, C. & Höfte, H. (2011) Pectin-induced changes in cell wall mechanics underlie organ initiation in *Arabidopsis*. *Current Biology*, 21, 1720–1726.
- Peaucelle, A., Louvet, R., Johansen, J.N., Höfte, H., Laufs, P., Pelloux, J. et al. (2008) *Arabidopsis* phyllotaxis is controlled by the methyl-esterification status of cell-wall pectins. *Current Biology*, 18, 1943–1948.
- Peters, A.J., Walter-Shea, E.A., Ji, L., Vina, A., Hayes, M. & Svoboda, M. D. (2002) Drought monitoring with NDVI-based standardized vegetation index. *Photogrammetric Engineering and Remote Sensing*, 68, 71–75.
- Portillo-Estrada, M., Zenone, T., Arriga, N. & Ceulemans, R. (2018) Contribution of volatile organic compound fluxes to the ecosystem carbon budget of a poplar short-rotation plantation. *Global change biology*, 10, 405–414.
- Ragauskas, A.J., Williams, C.K., Davison, B.H., Britovsek, G., Cairney, J., Eckert, C.A. et al. (2006) The path forward for biofuels and biomaterials. *Science*, 311, 484–489.
- Ramírez, V., Xiong, G., Mashiguchi, K., Yamaguchi, S. & Pauly, M. (2018) Growth- and stress-related defects associated with wall hypoacetylation are strigolactone-dependent. *Plant Direct*, 2, e00062.
- Ren, A., Ahmed, R.I., Chen, H., Han, L., Sun, J. & Ding, A. et al. (2019) Genome-wide identification, characterization and expression patterns of the pectin methyltransferase inhibitor genes in *Sorghum bicolor*. *Genes*, 10, 755.
- Roig-Oliver, M., Nadal, M., Clemente-Moreno, M.J., Bota, J. & Flexas, J. (2020) Cell wall components regulate photosynthesis and leaf water relations of *Vitis vinifera* cv. Grenache acclimated to contrasting environmental conditions. *Journal of Plant Physiology*, 244, 153084.
- Sannigrahi, P., Ragauskas, A.J. & Tuskan, G.A. (2010) Poplar as a feedstock for biofuels: a review of compositional characteristics. *Biofuels, Bioproducts and Biorefining*, 4, 209–226.
- Scheller, H.V. (2017) Plant cell wall: never too much acetate. *Nature Plants*, 3, 17024.
- Sechet, J., Htwe, S., Urbanowicz, B., Agyeman, A., Feng, W., Ishikawa, T. et al. (2018) Suppression of *Arabidopsis* GGLT1 affects growth by reducing the L-galactose content and borate cross-linking of

- rhamnogalacturonan-II. *The Plant Journal: For Cell and Molecular Biology*, 96, 1036–1050.
- de Souza, A., Hull, P.A., Gille, S. & Pauly, M. (2014) Identification and functional characterization of the distinct plant pectin esterases PAE8 and PAE9 and their deletion mutants. *Planta*, 240, 1123–1138.
- Su, L., Patton, E.G., Vilà-Guerau de Arellano, J., Guenther, A.B., Kaser, L., Yuan, B. et al. (2016) Understanding isoprene photooxidation using observations and modeling over a subtropical forest in the southeastern US. *Atmospheric Chemistry and Physics*, 16, 7725–7741.
- Sun, Y., Fu, R., Dickinson, R., Joiner, J., Frankenberg, C., Gu, L. et al. (2015) Drought onset mechanisms revealed by satellite solar-induced chlorophyll fluorescence: insights from two contrasting extreme events. *Journal of Geophysical Research: Biogeosciences*, 120, 2427–2440.
- Trueba, S., Pan, R., Scoffoni, C., John, G.P., Davis, S.D. & Sack, L. (2019) Thresholds for leaf damage due to dehydration: declines of hydraulic function, stomatal conductance and cellular integrity precede those for photochemistry. *The New Phytologist*, 223, 134–149.
- Urbanowicz, B.R., Peña, M.J., Moniz, H.A., Moremen, K.W., York, W.S. (2014) Two Arabidopsis proteins synthesize acetylated xylan in vitro. *The Plant Journal*, 80, 197–206.
- Wang, J., Ling, L., Cai, H. & Guo, C. (2020) Gene-wide identification and expression analysis of the PME1 family genes in soybean (*Glycine max*). *3 Biotech*, 10(8). <https://doi.org/10.1007/s13205-020-02328-9>
- Wei, Y., Lin, M., Oliver, D.J., & Schnable, P.S. (2009) The roles of aldehyde dehydrogenases (ALDHs) in the PDH bypass of Arabidopsis. *BMC Biochemistry*, 10, 1.
- Willats, W.G., McCartney, L., Mackie, W. & Knox, J.P. (2001) Pectin: cell biology and prospects for functional analysis. *Plant Molecular Biology*, 47, 9–27.
- Yuan, Y., Teng, Q., Zhong, R., Haghghat, M., Richardson, E.A. & Ye, Z.-H. (2016) Mutations of arabidopsis TBL32 and TBL33 affect xylan acetylation and secondary wall deposition. *PLoS One*, 11, e0146460.
- Zhong, R., Cui, D. & Ye, Z.-H. (2017) Regiospecific acetylation of xylan is mediated by a group of DUF231-containing O-Acetyltransferases. *Plant & Cell Physiology*, 58, 2126–2138.
- Zhou, J., Zhang, Z., Sun, G., Fang, X., Zha, T., McNulty, S. et al. (2013) Response of ecosystem carbon fluxes to drought events in a poplar plantation in Northern China. *Forest Ecology and Management*, 300, 33–42.

SUPPORTING INFORMATION

Additional supporting information can be found online in the Supporting Information section at the end of this article.

How to cite this article: Jardine, K.J., Dewhirst, R.A., Som, S., Lei, J., Tucker, E., Young, R.P. et al. (2022) Cell wall ester modifications and volatile emission signatures of plant response to abiotic stress. *Plant, Cell & Environment*, 45, 3429–3444. <https://doi.org/10.1111/pce.14464>